Spontaneous EEG alpha oscillation interacts with positive and negative BOLD responses in the visual–auditory cortices and default-mode network

Mayhew, Stephen D.; Ostwald, Dirk; Porcaro, Camillo; Bagshaw, Andrew P.

DOI:
10.1016/j.neuroimage.2013.02.070

Document Version
Publisher's PDF, also known as Version of record

Citation for published version (Harvard):
Mayhew, SD, Ostwald, D, Porcaro, C & Bagshaw, AP 2013, 'Spontaneous EEG alpha oscillation interacts with positive and negative BOLD responses in the visual–auditory cortices and default-mode network', *NeuroImage*, vol. 76, pp. 362-372. https://doi.org/10.1016/j.neuroimage.2013.02.070

NeuroImage 76 (2013) 362–372

Contents lists available at SciVerse ScienceDirect

NeuroImage

journal homepage: www.elsevier.com/locate/ynimg

Spontaneous EEG alpha oscillation interacts with positive and negative BOLD responses in the visual–auditory cortices and default-mode network

Stephen D. Mayhew [a,*], Dirk Ostwald [b], Camillo Porcaro [c,d], Andrew P. Bagshaw [a]

[a] School of Psychology and BUIC, University of Birmingham, Birmingham, UK
[b] Max Planck Institute for Human Development, Berlin, Germany
[c] LET'S ISTC-CNR, Rome, Italy
[d] Institute of Neuroscience, Newcastle University, Newcastle upon Tyne, UK

ARTICLE INFO

Article history:
Accepted 25 February 2013
Available online 15 March 2013

Keywords:
Single-trial
EEG–fMRI
Alpha
Negative BOLD
Default-mode network
Neuronal activity

ABSTRACT

The human brain is continually, dynamically active and spontaneous fluctuations in this activity play a functional role in affecting both behavioural and neuronal responses. However, the mechanisms through which this occurs remain poorly understood. Simultaneous EEG–fMRI is a promising technique to study how spontaneous activity modulates the brain's response to stimulation, as temporal indices of ongoing cortical excitability can be integrated with spatially localised evoked responses. Here we demonstrate an interaction between the ongoing power of the electrophysiological alpha oscillation and the magnitude of both positive (PBR) and negative (NBR) fMRI responses to two contrasts of visual checkerboard reversal. Furthermore, the amplitude of pre-stimulus EEG alpha-power significantly modulated the amplitude and shape of subsequent PBR and NBR to the visual stimulus. A nonlinear reduction of visual PBR and an enhancement of auditory NBR and default-mode network NBR were observed in trials preceded by high alpha-power. These modulated areas formed a functionally connected network during a separate resting-state recording. Our findings suggest that the "baseline" state of the brain exhibits considerable trial-to-trial variability which arises from fluctuations in the balance of cortical inhibition/excitation that are represented by respective increases/decreases in the power of the EEG alpha oscillation. The consequence of this spontaneous electrophysiological variability is modulated amplitudes of both PBR and NBR to stimulation. Fluctuations in alpha-power may subserve a functional relationship in the visual–auditory network, acting as mediator for both short and long-range cortical inhibition, the strength of which is represented in part by NBR.

Introduction

Recent work has demonstrated the fundamental importance of intrinsically connected networks (ICNs) of brain regions in supporting human brain function (Smith et al., 2009). Neuronal activity is strongly correlated between individual ICN nodes during the resting-state (De Luca et al., 2006). Individual components of these ICNs can be modulated by external inputs giving rise to the stimulus-evoked response that is the principal, non-invasive measure used to elucidate the spatial origin and intensity of brain activity with EEG and fMRI. Single-trial responses can be modulated by the brain's spontaneous activity (Arieli et al., 1996; Becker et al., 2011; Fox et al., 2007; Nierhaus et al., 2009) suggesting that interactions between ongoing network dynamics and processing of external events are intrinsic to the function of the brain. However the functional significance of these modulations and the neural substrates that give rise to them remains poorly understood.

Simultaneous EEG–fMRI allows the investigation of these dynamic interactions because temporal indices of ongoing brain activity can be extracted from EEG frequency bands and their origins spatially localised with fMRI. The dominant characteristic of scalp EEG is the 7–13 Hz alpha oscillation (Berger, 1929) which forms an important substrate of human cognition (Jensen and Mazaheri, 2010; Klimesch, 1997; Klimesch et al., 2007; Mathewson et al., 2011). Alpha functionality is characterised by phasic cycles where increases or decreases in the synchrony of the oscillation reflect states of inhibited or enhanced cortical excitability respectively (Anderson and Ding, 2011; Foxe et al., 1998; Pineda, 2005; Romei et al., 2008) that influence the detection and perception of external stimuli (Hanslmayr et al., 2007; Thut et al., 2006).

This study aims to clarify contrasting reports that the positive blood oxygenation level dependent (BOLD) fMRI response (PBR) to visual stimulation is unaffected (Scheeringa et al., 2011) or linearly modulated by pre-stimulus alpha-power (Becker et al., 2011). We extend previous work by investigating the alpha–BOLD relationship with varying stimulus intensity and in brain networks beyond visual cortex, including areas displaying a decrease in BOLD signal below pre-stimulus baseline levels (negative BOLD response (NBR)). Recent work emphasizes that the functional significance of alpha power is not restricted to visual

* Corresponding author at: School of Psychology, University of Birmingham, Edgbaston, Birmingham, B15 2TT, UK.
E-mail address: s.d.mayhew@bham.ac.uk (S.D. Mayhew).

1053-8119/$ – see front matter © 2013 Elsevier Inc. All rights reserved.
http://dx.doi.org/10.1016/j.neuroimage.2013.02.070

cortex and alpha can act as a top–down brain mechanism for shaping input information and controlling neuronal processing (Klimesch et al., 2007; Mathewson et al., 2011). As trial-by-trial analyses become increasingly utilised (Debener et al., 2006; Scheibe et al., 2010), it is important to understand to what extent evoked brain responses can be modulated by ongoing network activity. This will allow a clearer interpretation of whether differences in the single-trial brain response measured between experimental conditions are induced solely by the experimental paradigm or can be explained by variations in the state of the brain at the time of stimulation.

Visual tasks induce NBR in the unstimulated or unattended regions of visual cortex (Tootell et al., 1998), auditory cortex (Laurienti et al., 2002) and the default-mode network (DMN) (Singh and Fawcett, 2008). Though the neurophysiological origins of the NBR remain incompletely understood, NBR is associated with concurrent decreases in cerebral blood flow and oxygen metabolism and is thought to represent neuronal deactivation via functional inhibition of non task-related processing (Ferbert et al., 1992; Klingner et al., 2010; Shmuel et al., 2006). Investigating whether the NBR is modulated by spontaneous activity in a comparable manner to the PBR may help to elucidate the functional significance of and the physiological mechanisms underlying the NBR. Primary visual and auditory cortices demonstrate cross-modal influences, where activation in one stimulus modality suppresses activity in the other (Laurienti et al., 2002). These cortices share both structural and functional connections as demonstrated in both primates (Falchier et al., 2002; Rockland and Ojima, 2003) and humans (Beer et al., 2011; Eckert et al., 2008) which provides an underlying network substrate to facilitate this neuronal communication.

Here we use simultaneous EEG–fMRI to investigate the hypothesis that cortical alpha oscillations play a role in mediating the balance of excitation and inhibition and influence the magnitude of both PBR and NBR in the visuo-auditory and default-mode networks. We present a novel EEG–fMRI integration application of the general linear model (GLM) by explicitly modelling an index of ongoing cortical excitability (alpha-power) and its interaction with the brain response to stimulation. This approach demonstrates that the so-called “baseline” of brain activity can substantially modulate PBR and NBR across cortical regions both directly and indirectly driven by the task.

Materials and methods

Stimulation paradigm and data acquisition

Fourteen subjects participated in the experiment (4 female, 27.8 ± 5.4 years, (mean ± std)). Written, informed consent was obtained from all participants and the protocol was approved by the Research Ethics Board of the University of Birmingham. As described in initial methodological publications (Ostwald et al., 2010, 2011; Porcaro et al., 2010) left visual hemi-field, checkerboard stimuli were presented for one second, separated by an inter-stimulus interval of either 16.5, 19 or 21 s to allow haemodynamic responses to recover to baseline between stimuli. Black/white checkerboard stimuli were presented at either high ($C_{Michelson} = 1$) or low ($C_{Michelson} = 0.25$) contrast levels in a pseudo-randomized order. Five experimental runs were acquired in each participant, each consisting of 17 trials per contrast, providing 85 trials per contrast in total. Subjects were instructed to continually fixate on a central fixation cross that was displayed throughout. A simple fixation task was performed to ensure maintenance of central fixation and subject's attention: in a random selection of half of the trials, the fixation cross changed from a plus sign to an X at a random point during the fixation period uniformly sampled from the interval of 4.5–16.5 s after stimulus onset. Subjects reported the change in fixation by a button press using the index finger of the right hand. In parallel with the visual stimulation, simultaneous EEG–fMRI data were acquired using a 3 T Philips Achieva MRI scanner equipped with an eight-channel, phased array head coil and a 64-channel MR compatible EEG system (Brain Products, Germany). EPI data were acquired from 20 slices (441 volumes, 2.5 × 2.5 × 3 mm, TR = 1500 ms, TE = 35 ms, SENSE factor = 2, flip angle = 80°), providing approximately half-brain coverage in the dorsal–ventral direction. Individual runs were separated by a short period (maximum of 2 min) to minimise subject fatigue. Additionally, a high-resolution (1 mm isotropic) T1-weighted anatomical image was acquired. EEG data were recorded from 62 Ag/AgCl ring-type scalp electrodes, distributed according to the 10–20 system, with two additional channels used for recording the ECG and electrooculogram (EasyCap, Herrsching, Germany). EEG data were sampled at 5 kHz, synchronised with the MRI scanner clock (Mullinger et al., 2008), with hardware filters of 0.016–250 Hz. Impedance at all recording electrodes was maintained below 20 kΩ. In addition to the visual stimulation runs, a 3-minute resting scan was acquired (120 volumes). Participants were instructed to close their eyes and think of nothing in particular. Total duration of data acquisition was sixty minutes.

Data analysis

EEG processing

The gradient and pulse artefacts were removed using average-artefact subtraction in Brain Vision Analyzer 1.05 (Brain Products, Munich, Germany) and optimal basis sets (Niazy et al., 2005) respectively. Separately for each subject, data from all stimulus runs were concatenated and down-sampled to 500 Hz. These data were then band-pass filtered into separate visual evoked potential (VEP, 1–25 Hz) and alpha (7–13 Hz) datasets.

VEP extraction

Functional source separation (FSS) was applied to the VEP data as a second EEG processing step. FSS, a semi-blind extension of the independent component analysis (ICA) technique, has recently been demonstrated to reliably improve single-trial EEG data recorded during concurrent EEG–fMRI (Ostwald et al., 2010; Porcaro et al., 2010). We implemented FSS incorporating prior knowledge about the response of interest, here the P100 peak latency, to provide improved extraction of the neuronal source generating the stimulus response as described in detail in Porcaro et al. (2010). The FSS source was then retro-projected to obtain its electric potential distribution at the scalp electrodes to facilitate integration of VEP measurements with alpha power analysis that was conducted at the channel level (see below). High (HC) and low (LC) contrast single-trial VEPs were extracted from electrode PO8 (−200 ms to +500 ms relative to stimulus onset) and corrected for pre-stimulus baseline. Single-trial P100–N140 amplitudes were measured (Mayhew et al., 2006).

Measuring occipital alpha-power

To optimize the extraction of alpha-frequency neuronal oscillations, a semi-automatic ICA (fastICA, (Hyvarinen, 1999)) feature selection was performed on the 7–13 Hz alpha-band filtered data. Only components displaying bilateral, occipital scalp topography and clear spectral peak presenting alpha-power were retained. ICs that contained signal time-locked to the stimulus were excluded to maximise the separation of the ongoing alpha oscillation from the lateralized evoked response, as although VEPs represent functionally distinct brain processes to the alpha oscillation, the power of the VEP response could confound the measurement of ongoing alpha, which was our priority. No lateralized components were rejected that contained only alpha frequency signals. We focus our analysis upon bilateral alpha power, which provides a reliable measure of visual network excitability and best enables us to investigate the bilateral modulation of BOLD responses both within and beyond visual cortical areas. Following component selection, data were retro-projected into channel space and channels PO3/4, POz, O1/2 and Oz were epoched using: 1) the MRI volume acquisition onset timings (‘TR epochs’); 2) −1000 ms to +4000 ms peri-stimulus time window (‘stimulus epochs’). Time–frequency spectrograms of oscillatory power

were separately calculated for all TR and stimulus epochs using the continuous Morlet wavelet transform in the Fieldtrip toolbox (http://fieldtrip.fcdonders.nl/) (Oostenveld et al., 2011).

Continuous alpha-power for general-linear model analysis

Using a ±1 Hz interval around each individual's alpha frequency (IAF) the mean alpha-power was calculated for each TR epoch, sub-sampling continuous alpha-power at the temporal resolution of fMRI, averaged across channels and mean subtracted. Alpha-power was then normalised to control for differences in maximum alpha-power between subjects and for each run an alpha time-series regressor was calculated for subsequent GLM analysis of fMRI data.

Stimulus-induced changes in alpha-power

For each stimulus epoch, the timecourses of the alpha response induced by HC and LC stimuli were extracted from the IAF ±1 Hz lines of each spectrogram and normalised across subjects.

Pre-stimulus alpha-power

The mean pre-stimulus alpha-power (−500 ms to 0 ms) was calculated from the spectrogram of each stimulus trial using a ±1 Hz interval around the IAF.

Evaluation of VEP and alpha responses to visual stimulation

Separately for HC and LC stimuli, induced alpha and evoked VEP response trials were subsequently sorted into lower and upper 25% quartiles of pre-stimulus alpha-power. For each subject, single-trial P100–N140 amplitudes were averaged within lower and upper quartiles and a paired t-test was used to test for P100–N140 amplitude differences between quartiles across the group. Similarly, alpha-power timecourses were averaged within quartiles and the exact temporal period of differences between quartiles was then tested using paired t-tests at each time point across the group. Finally, spectrograms were averaged across all trials and subjects to create a group representation of stimulus induced changes in oscillatory alpha-power.

fMRI pre-processing

All fMRI analyses were carried out using FSL 4.1.8 (FMRIB's Software Library, www.fmrib.ox.ac.uk/fsl). The following pre-processing was applied: automated brain extraction using BET (Smith, 2002), motion correction using MCFLIRT (Jenkinson et al., 2002), slice-timing correction, spatial smoothing using a Gaussian kernel (5 mm FWHM), and high-pass temporal filtering (>0.01 Hz). Registration to high-resolution structural and MNI standard brain images was carried out using FLIRT (Jenkinson and Smith, 2001). Data from three subjects was subsequently discarded due to multiple movements >3 mm identified from the MRI motion parameters that resulted in poor quality of both EEG and fMRI data.

EEG–fMRI integration

Regional inference was carried out in the GLM framework. We were interested in identifying brain areas where the BOLD response was significantly modulated by visual stimulation, visual stimulus contrast, and spontaneous alpha-power. Additionally, we sought to characterise the brain areas in which differential BOLD responses to visual stimulus contrast were modulated by alpha-power. This motivated us to employ a GLM design analogous to the psychophysiological interaction (PPI) method (Friston et al., 1997; O'Reilly et al., 2012). More traditionally, these designs are referred to as Analysis of Covariance (ANCOVA) with interaction and classically embody one discrete factor (here visual stimulus contrast with two factor levels, LC and HC) and one continuous factor (here alpha-power) and their interaction. The first-level (i.e. run specific) design matrices thus comprised four regressors: 1) main effect of visual stimulation, constant amplitude Dirac δ-functions located at the onset of each stimulus; 2) main effect of visual stimulus contrast, constant amplitude Dirac δ-functions located at the onset of HC stimuli

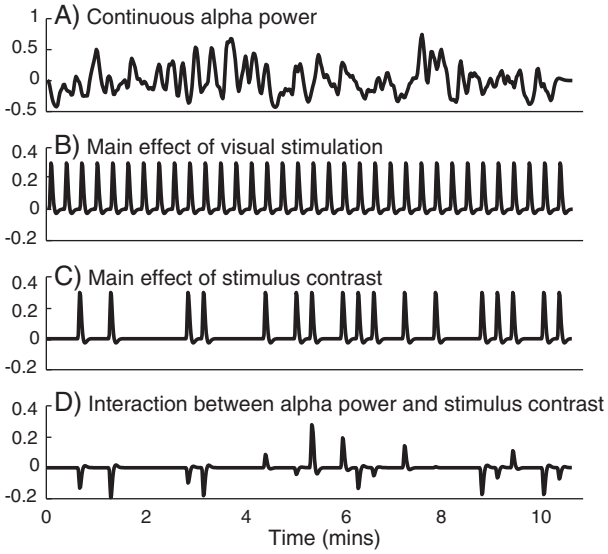

Fig. 1. Graphical time-series representation of an example first-level design matrix comprising four regressors convolved with the canonical HRF: main effects of continuous alpha power A), visual stimulation B), visual contrast C) and the interaction between alpha-power and visual contrast D). The amplitude and polarity of D) was determined by the state of the alpha oscillation.

only; 3) main effect of continuous alpha-power derived from the EEG data as described above; and 4) the interaction between continuous alpha-power and visual contrast, modelled as the element-wise multiplication of columns (2) and (3). The multiplication of the constant amplitude contrast regressor with the alpha-power creates an additional regressor, the amplitude of which is non-linearly larger when a stimulus occurs during a state of high alpha-power and smaller when a stimulus occurs during low alpha-power. All regressors were convolved with a canonical double-gamma HRF and positive and negative contrasts were assessed for all regressors. A representative first-level design matrix is shown in Fig. 1. Simulations were performed to test the statistical power and validity of our design matrix (see Supplementary information). Figs. S1, S2 and S3 demonstrate that each condition of interest in the simulated data (all main effects and the interaction term) is separately detected by its designated regressor without affecting the fit of the rest of the model. No systematic bias is observed in any of the beta weights, demonstrating that the design matrix is sound and non-rank deficient. Statistical analysis was carried out in FEAT 5.98 using FILM with local autocorrelation correction (Woolrich et al., 2001). First-level results were combined across all runs to calculate an average response per subject at the second-level with fixed effects and then combined across all subjects at the third-level using FLAME 1 + 2 mixed effects (Woolrich et al., 2004). All Z-statistic images were thresholded using clusters determined by a $Z > 2.0$ and cluster corrected significance threshold of $p < 0.05$.

ROI definition and timecourse extraction

EEG–fMRI integration was used to identify brain regions exhibiting an alpha–BOLD interaction, based on fitting a canonical HRF to BOLD responses in a GLM analysis framework. We further visualized the temporal characteristics of the alpha-dependent modulation upon the regional PBR and NBR timecourses by examining the differences in response shape and area, rather than just amplitude, which are dependent upon spontaneous brain activity. The intrinsic negative coupling between alpha and BOLD signals was controlled for by removing the weighting of continuous alpha-power from each voxel of the BOLD data using multiple linear regression in the fsl_regfilt tool. Additionally, we examine the effect of pre-stimulus alpha power on the residuals of the GLM fit, investigating the alpha-modulation of the remaining BOLD response variance after all

main effects and the interaction term are removed from the data. Single-trial haemodynamic responses (HRs) were then extracted from visual, auditory and default-mode network (DMN) regions of interest (ROIs). ROIs were defined by centering a 3 × 3 × 3 voxel cube (7.5 × 7.5 × 9 mm) on the maximum Z-statistic voxel of the following group-level GLM contrasts:

1) Stimulus PBR: Defined from the main effect of visual stimulation > baseline in contralateral visual cortex and separately in the contralateral lateral geniculate nucleus (LGN).
2) Stimulus NBR: Defined from the main effect of visual stimulation < baseline in bilateral auditory cortex and separately in the precuneus/posterior cingulate (PCC).
3) Continuous alpha-power: Defined from the negative correlation between continuous alpha and BOLD signal in ipsilateral primary visual cortex.
4) Alpha–BOLD interaction in PBR regions: Defined from the conjunction between the stimulus–alpha interaction and visual stimulation > baseline in visual cortex.
5) Alpha–BOLD interaction in NBR regions: Defined from the conjunction between the stimulus–alpha interaction and visual stimulation < baseline, separately in auditory cortex and PCC.

All ROIs were registered to individual runs and the average voxel timecourse was extracted. Timecourses were epoched based upon stimulus timings (−2 to +11 sample points) to create single-trial HRs separately for HC and LC stimuli. Separately for each run and each ROI, the mean HR was calculated across both HC and LC stimuli and the average value of the first three time-points was taken as the signal baseline level for that run. Using all data in this manner ensured that potential baseline differences between HC and LC conditions could not confound subsequent analyses. Single-trial HRs were then converted into percent signal change relative to this baseline level. For each ROI, separately for each subject, single-trial HRs were sorted into lower and upper quartiles based upon the amplitude of pre-stimulus alpha-power in the corresponding EEG trial. Lower and upper quartile HRs were averaged across subjects, separately for both HC and LC stimuli, and the integral of HR area was calculated. For each ROI, paired student's t-test was used to identify time-points with differences in HR amplitude between quartiles.

Resting-state analysis

Functional connectivity analyses (fcMRI) were conducted to investigate the properties of the visual–auditory network and the DMN during the resting-state. Our motivation for this was to investigate whether regions that displayed a modulation of BOLD response with alpha power during the task exhibited intrinsic coherence in the fluctuations of resting-state BOLD signal which is indicative of a functionally connected network. Firstly, resting-state data from all subjects were temporally concatenated and MELODIC was used to decompose this group data into 10 maximally independent spatial maps (Beckmann and Smith, 2004). This relatively low number of components was chosen to ensure that the entire DMN network was encapsulated by a single component rather than fractured into individual areas between several components. A single group DMN component was manually identified based on its characteristic spatial pattern of PCC, bilateral intra-parietal lobe and medial prefrontal cortex (mPFC) (De Luca et al., 2006; Raichle et al., 2001). Secondly, the resting-state data from each subject were low-pass filtered ($0.008 < f < 0.08$ Hz) and the following trends of no-interest were removed with linear regression: six motion parameters, ventricular, white-matter and global brain signals (Fox et al., 2005). An MNI standard-space mask of bilateral Heschl's gyrus (Harvard–Oxford cortical structural atlas) was applied to the group-level statistical GLM map of the significant alpha–BOLD interaction to define an auditory seed ROI for fcMRI. First-level, voxel-wise correlations with the mean seed timecourse were combined across subjects at the second-level with fixed effects using FEAT ($p < 0.05$ cluster corrected).

Results

Behavioural data

Due to a technical malfunction of the response device, behavioural data were only obtained from eight subjects. For these, the hit rate in the target detection task was high (0.95 ± 0.03 (SEM)) and the number of false alarms was low (3.1 ± 1.6 (SEM)) indicating good task performance, and maintenance of central fixation and attention throughout.

EEG

Simultaneous EEG–fMRI recordings suffer from the detrimental effects of MR environment artefacts on EEG data quality (Mullinger and Bowtell, 2011). To ensure that the EEG data processing maintained the neuronal signals of interest whilst suppressing artefactual components, we analysed the EEG time–frequency and evoked potential stimulus response features and their modulation by pre-stimulus alpha-power. In accordance with previous studies (Brookes et al., 2005; Woertz et al., 2004) the group mean time–frequency spectrograms showed that visual stimuli induced a non-phase locked alpha event-related desynchronisation (ERD) in all subjects, for HC (Fig. 2A) and LC (Fig. 2B), lasting between 0.1 and 1.3 s post-stimulus, coincident with the stimulus presentation. The ERD was followed by a pronounced alpha rebound from 2.1 to 4 s. In all subjects ICs representing continuous alpha-power (7.3 ± 2.4 mean ± std) were identified. The group average, bilateral occipital scalp topography of alpha-power is shown in Fig. 2C. Robust, phase-locked VEP responses with contralateral, occipital scalp topographies were also measured in all subjects. In analogy with previous studies (Becker et al., 2008; Reinacher et al., 2009), a significant effect of pre-stimulus alpha-power upon both ERD (Fig. 2D and E) and VEP (Fig. 2F and G) amplitudes was observed. Specifically, higher pre-stimulus alpha-power indexed trials with larger VEP P100–N140 amplitude and larger magnitude ERD. These results indicate that our EEG pre-processing has preserved the neuronal signals of interest whilst suppressing artefacts, allowing us to identify subtle effects of pre-stimulus alpha rhythm on post-stimulus alpha-power and the VEP.

EEG–fMRI GLM

Group mixed-effect statistical maps showed that the main effect of left-hemifield checkerboard stimulation evoked significant PBR in contralateral (right) LGN, contralateral V1 (cV1) and bilateral secondary visual areas (Fig. 3, red). Significant NBR to visual stimulation was observed in bilateral auditory cortex as well as the PCC and mPFC (Fig. 3, dark blue) (see Table 1 for MNI co-ordinates). The amplitude of continuous occipital alpha-power correlated negatively with BOLD signal in bilateral primary and secondary visual cortices (Fig. 3, light blue). A significant negative interaction between the amplitude of alpha-power and visual stimulus contrast (Fig. 3, green) was observed bilaterally in anterior primary visual and primary auditory cortices, as well as the PCC. Substantial overlap between the stimulus PBR and this interaction term was observed in anterior cV1 (Fig. 3, yellow, 634 voxels) and contralateral LGN; and between the stimulus NBR and the interaction in bilateral auditory cortex, PCC and mPFC (Fig. 3, purple, 1876 voxels). The main effect of visual contrast showed PBR and NBR in a subset of the visual, auditory and PCC regions activated by the main effects of stimulation (data not shown). No significant positive correlations with continuous alpha-power or positive interactions between alpha and stimulus contrast were observed.

To highlight in more detail the effects demonstrated by the GLM analysis, the BOLD HRs in Fig. 4 illustrate the regional modulation of the shape and area of both the PBR and NBR in relation to pre-stimulus alpha-power. No significant difference in PBR amplitude or area between

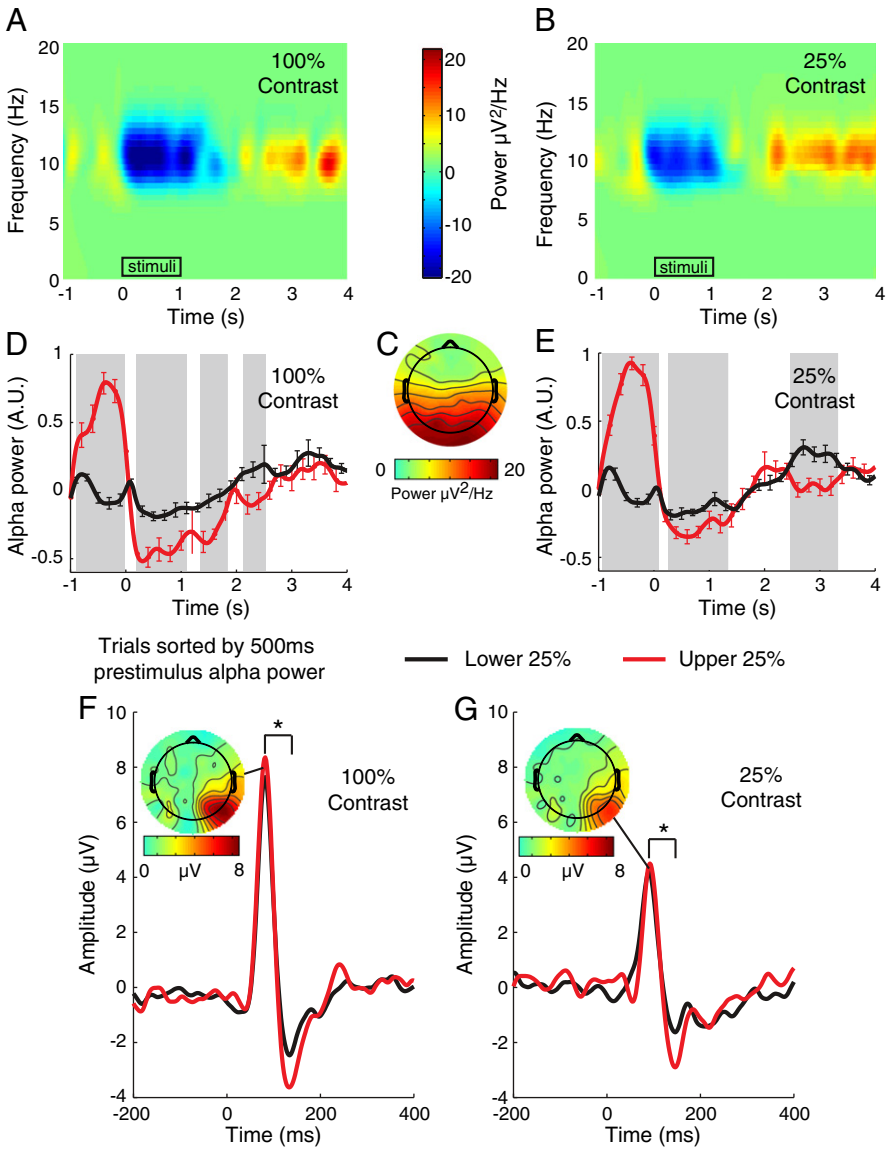

Fig. 2. Group average time–frequency spectrograms of HC (A) and LC (B) stimulus induced alpha response with group average bilateral scalp topography of occipital alpha-power (C). Black rectangles denote duration of stimulation. Effect of pre-stimulus alpha-power on the HC (D) and LC (E) alpha-power timecourse and HC (F) and LC (G) VEPs. Black and red lines denote lower and upper quartiles of pre-stimulus alpha-power respectfully. Grey shading denotes significant difference ($p < 0.05$) in amplitude between quartiles. Error bars represent standard error in the mean. * denotes significant ($p < 0.05$) difference in VEP P100–N140 amplitude between quartiles.

upper and lower quartiles of pre-stimulus alpha-power trials was observed in the peak-voxel ROI in posterior cV1 (Fig. 4A). However, the peak amplitude and area of PBR from anterior cV1 were significantly larger when visual stimuli were delivered during a state of low alpha-power than when stimulation occurred at high alpha-power (Fig. 4B) for both HC (6–10.5 s) and LC (6 s) stimuli. Similarly, when visual stimulation was delivered during the lower quartile of pre-stimulus alpha-power a small but significantly larger PBR in ipsilateral V1 (iV1) (HC 6–7.5 s, LC 4.5–6 s) was observed than when stimulation was delivered during the upper quartile (Fig. 4C). PBR in the contralateral LGN (Fig. 4D) was also larger in lower alpha quartile trials for the HC stimuli only (6 s and 10.5–12 s). The peak magnitude of the NBR in auditory cortex (Fig. 4E) and PCC (Fig. 4F) was increased (i.e. NBR was more negative) when visual stimuli were delivered at a state of high alpha-power compared to when stimulation occurred at low alpha-power. This effect lasted from 5 to 9 s for HC stimuli in both auditory and PCC and at 4.5 s for LC stimuli in auditory cortex. The distribution of upper and lower quartile trials was not significantly different between runs, so potential confounding effects of trial order within the experiment cannot account for the observed effects on HRs. Supplementary Fig. 4 shows that the residual BOLD response variance is significantly modulated by the alpha-power preceding stimulation. BOLD responses in anterior contralateral V1, ipsilateral V1 and auditory cortices are significantly modulated by pre-stimulus alpha power. This result further demonstrates that BOLD response variability over and above that which can be explained by the main effects of stimulation, alpha power and the interaction between alpha and stimulation, is dependent upon spontaneous brain activity.

Resting-state functional connectivity analyses

GLM analysis demonstrated alpha–BOLD interactions to the visual stimulus within auditory and visual cortex and also the PCC and mPFC (Fig. 3). We investigated whether these spatially distributed brain regions form functionally connected networks during the resting-state using the independent resting dataset acquired in each subject. Fig. 5 illustrates the very high degree of spatial overlap that we observe between the resting-state DMN identified using group ICA and the PCC and mPFC regions that display a significant NBR to visual stimulation.

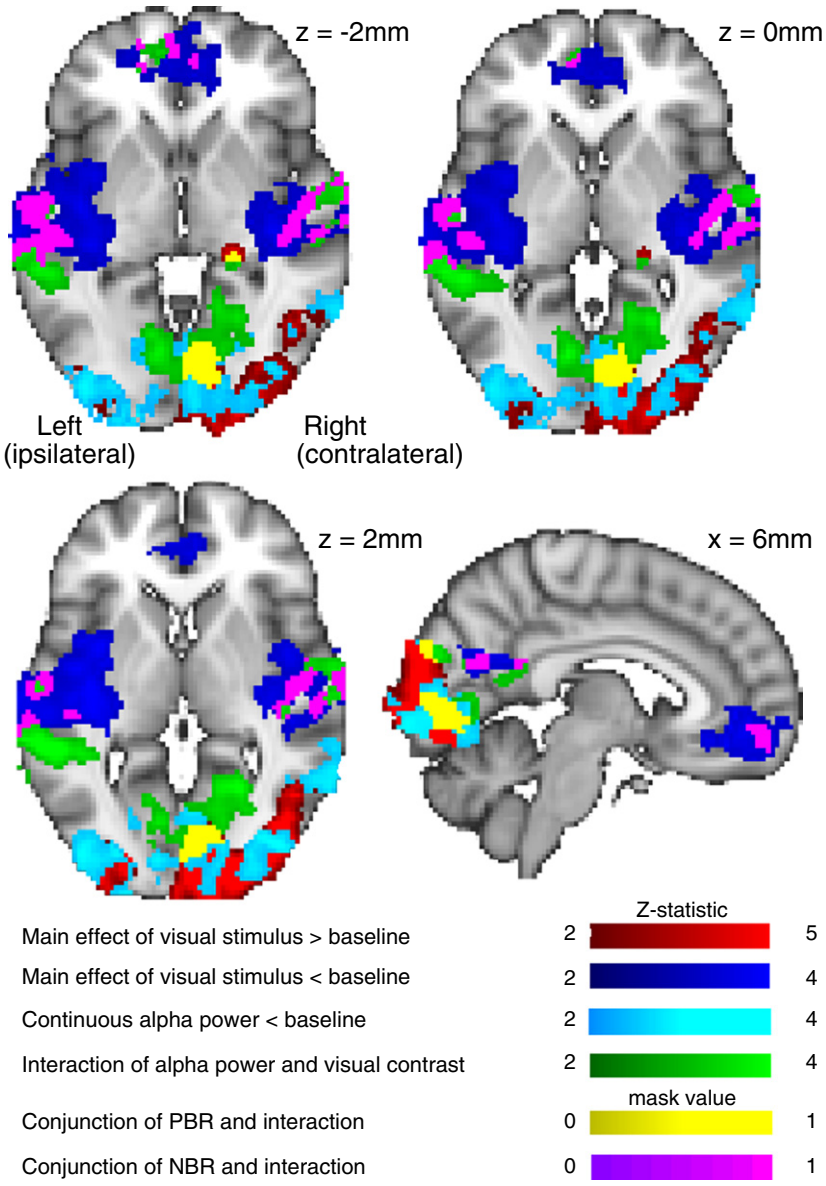

Fig. 3. Mixed effects group Z-statistic maps (all cluster corrected $Z > 2.0$, $p < 0.05$) of EEG–fMRI GLM results. Positive (red) and negative (dark blue) BOLD responses to constant amplitude main effect of visual stimulation overlaid with negative correlation between BOLD signal and continuous alpha-power (light blue). A significant negative interaction between continuous alpha-power and the main effect of visual stimulus contrast was observed (green) in visual and auditory cortices, precuneus and mPFC. The conjunction of the interaction with visual cortex positive BOLD regions is shown in yellow, and with auditory and DMN negative BOLD regions in purple.

Seed-based fcMRI analysis demonstrated that significant functional connectivity existed between primary auditory cortex and anterior primary visual cortex during the resting state (Fig. 6). Furthermore, a high degree of spatial overlap was observed between this functionally connected network at rest and the areas where a significant interaction between pre-stimulus alpha-power and both PBR and NBR was observed during stimulation (Fig. 6). The conjunction between areas exhibiting significant resting-state functional connectivity and alpha–BOLD interaction during visual stimulation comprised 3345 voxels.

Table 1
MNI co-ordinates of the peak Z-statistic voxel for the ROIs defined from the GLM analyses from primary visual (V1), LGN, primary auditory (A1) and DMN regions.

ROIs	MNI co-ordinates of peak voxel		
	X	Y	Z
Contralateral V1 PBR	6	−92	2
Contralateral V1 conjunction of PBR and alpha interaction	8	−76	−2
Contralateral LGN conjunction with alpha interaction	−18	−32	−2
Negative alpha-power correlation in contralateral V1	4	−94	−6
Negative alpha-power correlation in ipsilateral V1	−38	−90	−6
Contralateral A1 conjunction of NBR with alpha interaction	46	−22	2
Ipsilateral A1 conjunction of NBR with alpha interaction	−38	−22	6
PCC conjunction of NBR with alpha interaction	2	−66	24
mPFC conjunction of NBR with alpha interaction	2	48	−10

Discussion

This study significantly advances our understanding of the relationship between the spontaneous state of the brain and the brain's response to stimulation in several ways. We present a simple yet powerful method for investigating the modulation of fMRI responses by spontaneous brain activity by incorporating EEG alpha power, as a continuous index of cortical excitability (Romei et al., 2008), into the GLM and modelling its interaction with a conventional stimulus regressor. We present novel evidence of a significant interaction between the power of the ongoing alpha-oscillation and the BOLD response to visual contrast, suggesting

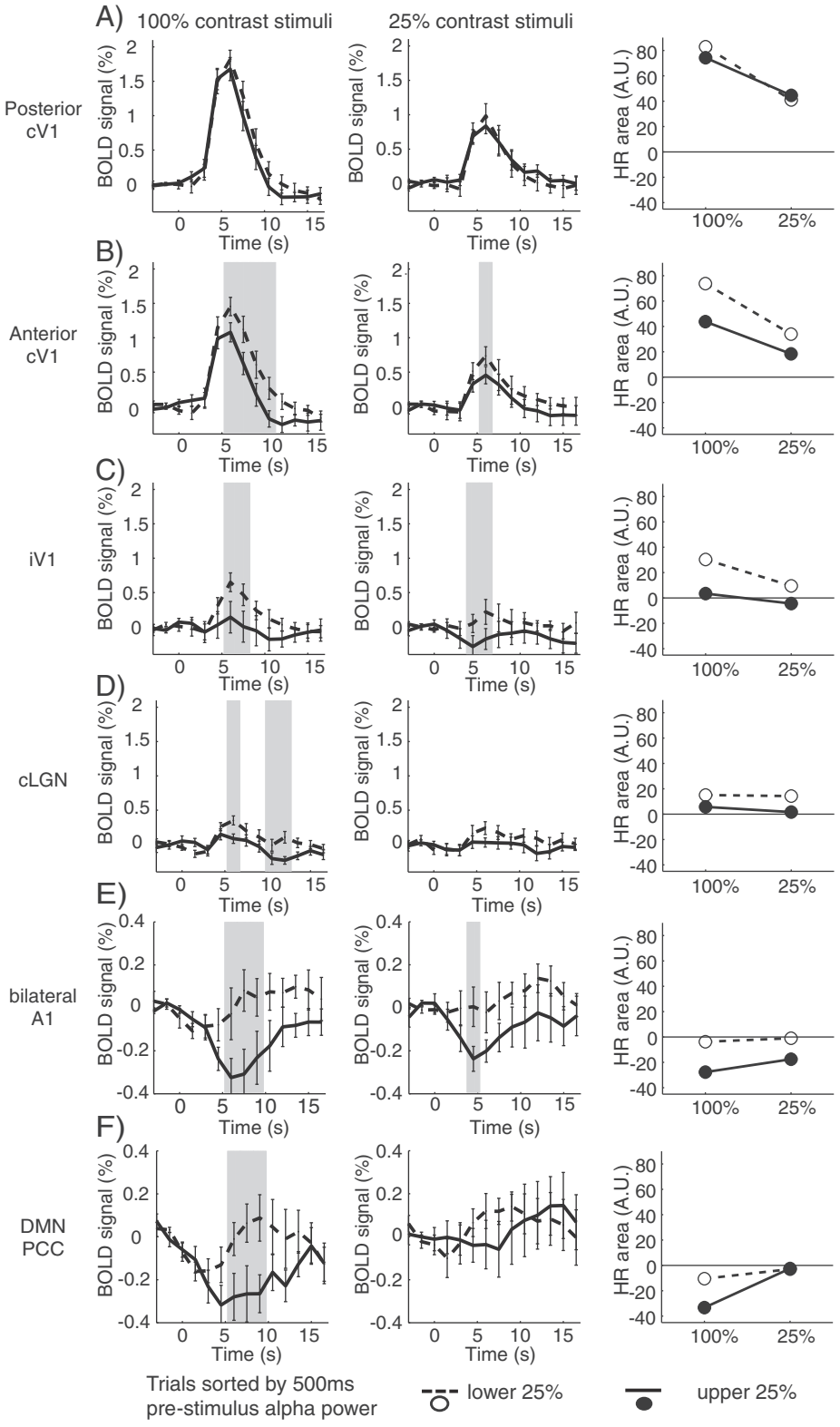

Fig. 4. Effect of pre-stimulus alpha-power on group average HR timecourses extracted from the following ROIs: Peak-voxel contralateral V1 PBR (A); conjunction of interaction with: anterior contralateral V1 PBR (B); negative BOLD and continuous alpha-power correlation in ipsilateral visual cortex (C); contralateral LGN PBR (D); bilateral auditory NBR (E); PCC NBR (F). Average of trials from lower (dashed line) and upper (thick line) quartiles of pre-stimulus alpha-power for HC (left column) and LC stimuli (right column). Grey shaded areas show time-points of significant difference ($p < 0.05$, paired t-test) in BOLD HR amplitude between lower and upper quartiles. Error bars represent ±standard error of the mean. Far right column plots the mean area of the HR for the lower and upper quartiles of both HC and LC trials.

that the dependency of the BOLD response upon the spontaneous state of the brain is related to the intensity of stimulation. The amplitude of pre-stimulus EEG alpha-power significantly modulates both the peak amplitude and the shape of positive and negative BOLD responses to visual stimulation. This alpha power modulation of the BOLD response amplitude is similar in both PBR and NBR regions. States of lower spontaneous

alpha power are associated with higher BOLD signal levels, which manifest as enhanced PBR and reduced NBR magnitudes.

Although we delivered a unilateral stimulus, the alpha modulation of BOLD responses is observed bilaterally in visual and auditory cortices and also in the midline nodes of the DMN. These distinct brain areas received very different stimulus-input information, display different BOLD response morphologies and polarities but are similarly modulated by alpha-power. The visuo-auditory areas are shown to form a functionally connected network in the resting state. Therefore we hypothesize that the observed BOLD modulation is a representation of top–down inhibitory control mechanisms in this network, indexed by the alpha oscillation (Klimesch et al., 2007). Our findings provide further support for the theory that reduced alpha-power indexes greater cortical excitability (Romei et al., 2008) and an enhanced response to stimulation (represented by increased PBR magnitude), whilst high alpha-power mediates inhibition (Jensen and Mazaheri, 2010) (represented by decreased PBR or increased NBR magnitude). Furthermore we provide novel evidence that this alpha modulation is not restricted to the directly stimulus-driven primary visual areas, but is associated with modulated NBR in other sensory modalities and in a general brain network such as the DMN. We suggest that this modulation of NBR occurs via fluctuations in the balance of cortical excitation/inhibition similar to the mechanism that underlies modulations of PBR.

Low pre-stimulus alpha-power enhances PBR to visual stimulation in visual cortex

Significantly increased PBR amplitude was associated with low alpha-power in anterior V1 but not in posterior contralateral V1 where the most significant BOLD response to the stimulus was observed. The powerful modulating effect of pre-stimulus alpha-power upon the BOLD response is particularly evident in ipsilateral V1, which was not directly stimulated by the hemifield checkerboard. iV1 exhibits a significant PBR when HC trials are preceded by low pre-stimulus alpha-power (i.e. at a period of high cortical excitability), but a negligible response when pre-stimulus alpha-power is high (Fig. 4C). For the LC stimulation, the pre-stimulus alpha-power predicts whether a PBR or an NBR is observed in iV1. This demonstrates that the BOLD response in iV1 displays a high degree of trial-to-trial variability and that spontaneous activity can be an important factor in determining response presence, polarity and magnitude.

A significant modulation of PBR in the contralateral LGN by pre-stimulus alpha-power was also observed (Fig. 4D). LGN thalamocortical neurons play a role in generating cortical alpha oscillations (Hughes et al., 2004; Lorincz et al., 2009). The LGN represents the first stage in the visual pathway at which top–down cortical feedback signals can affect processing (Kastner et al., 2006), and fMRI signal in the LGN has previously been shown to increase with stimulus contrast and be modulated by direction of attention, analogous to responses in visual cortex (O'Connor et al., 2002). The current data suggests that in an analogous manner to visual cortex, LGN excitability, as indexed by cortical alpha-power, is related to the amplitude of its response to stimulation.

Comparison with recent investigations of alpha–BOLD coupling

Recent studies have reported either no effect (Scheeringa et al., 2011) or a linear effect of alpha-power upon visual PBR (Becker et al., 2011). The present study suggests that in addition to linear alpha–BOLD coupling, significant BOLD response variance exists which can be explained by non-linear alpha–BOLD coupling. Our PPI–GLM demonstrates an interaction between alpha-power and the BOLD response to stimulation that is dependent upon the stimulus contrast. The current investigation of the relationship between alpha-power and PBR and NBR in visual, auditory and DMN regions, and the effect of stimulus intensity, extends previous studies that focussed exclusively on visual cortex and did not modulate stimulus input.

Becker et al., demonstrate a strong linear relationship between alpha and BOLD in visual cortex (Becker et al., 2011), however they did not test explicitly for non-linear effects. Scheeringa et al., show a linear modulation of BOLD by alpha power (in addition to alpha phase) but their subtraction of pseudo-trial activity from stimulus trials removes this effect (Scheeringa et al., 2011). The pseudo-trial approach is sub-optimal as it assumes: 1) temporal stationarity of alpha–BOLD coupling between the visual-fixation, baseline periods (defined as pseudo trials) and the stimulus trials at independent time points; 2) spatial stationarity of alpha–BOLD coupling; and 3) that alpha–BOLD coupling is equivalent during "rest" and during stimulation. In the current study, these assumptions would need to be extended to assume that the alpha–BOLD coupling is equivalent between rest and different stimulus intensities. Providing some evidence against these assumptions, Becker et al. calculate that a comparable alpha–BOLD coupling between rest and during stimulation exists in only a subset of occipital areas (Becker et al., 2011). Modelling the ongoing effect of alpha power at each fMRI time-point, as adopted in the current study and Becker et al., contains fewer assumptions about alpha–BOLD coupling and appears a more robust way of accounting for the spontaneously dynamic state of the brain, under the limits of the MR sampling frequency. Additionally, the magnitude of the BOLD responses measured in Scheeringa et al., is relatively small (~0.3%) (Scheeringa et al., 2011) compared to those reported here (~1.5%). The magnitude of the BOLD response is known to increase with increasing duration and/or intensity of visual stimulation (Shmuel et al., 2002). The alpha power modulation could potentially depend upon the size of the neuronal population recruited or the intensity of

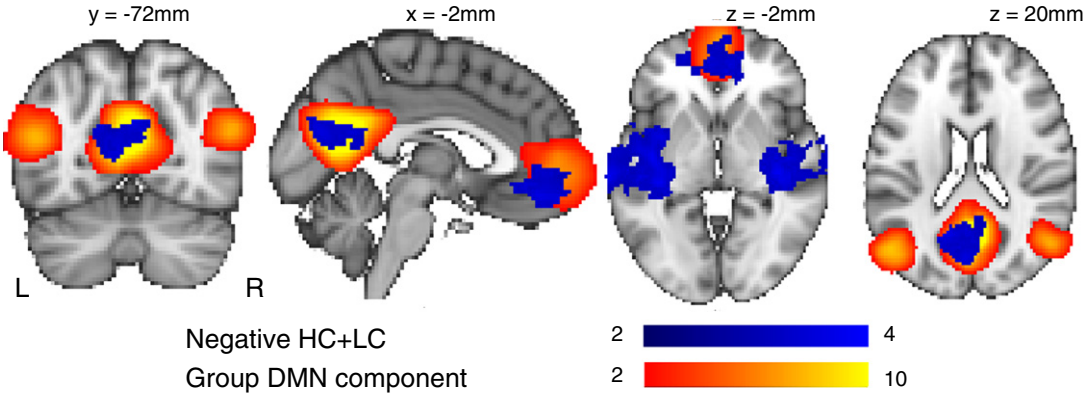

Fig. 5. Spatial relationship between the group average NBR to the visual stimulus (blue) in precuneus and mPFC and the group DMN (red–yellow) identified using group ICA of resting-state data.

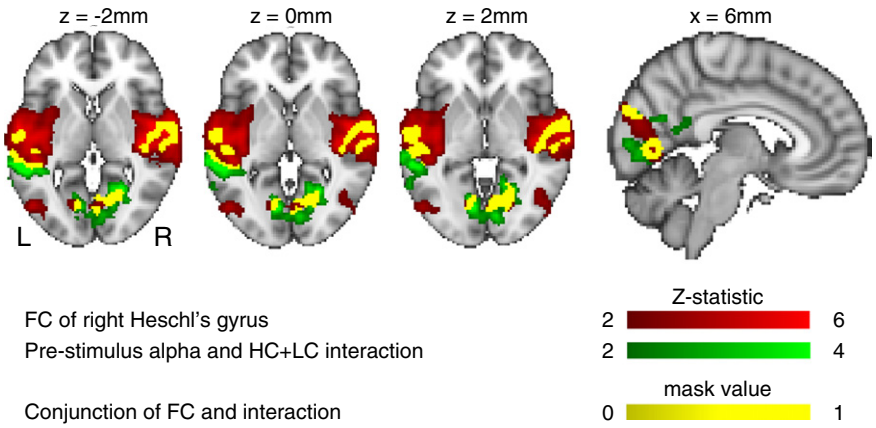

Fig. 6. Spatial relationship between visual–auditory networks defined at rest and during stimulation. Group average resting-state functional connectivity, seeded from right primary auditory cortex (red) is displayed with the regions of significant interaction between alpha-power and the BOLD response to visual stimulus contrast (green). The conjunction of the two maps is displayed in yellow.

the activity evoked by the stimulus. Therefore a further potential source of discrepancy between Scheeringa et al., and Becker et al., and the current study could lie in the duration of stimulation delivered (17 ms duration (Scheeringa et al., 2011) compared to 900 ms (Becker et al., 2011) and 1000 ms in the present study).

Functional interpretation of the alpha modulation of BOLD responses

The modulatory effect of pre-stimulus alpha-power extends into auditory and DMN regions where the BOLD signal is reduced below baseline in response to visual stimulation. During trials with low pre-stimulus alpha-power, NBR in both auditory and DMN ROIs is reduced in both magnitude and area and also peak at their maximum signal magnitude at an earlier latency (Fig. 4E,F). We therefore observe that during a state of low alpha power enhanced visual PBR is concurrent with reduced magnitude NBR and vice versa. The modulation of both PBR and NBR by alpha-power is suggestive of an underlying balance between excitatory and inhibitory drives across the entire network.

The increase and decrease of power in the alpha oscillation reflect concurrent increases and decreases in the synchronous firing of the underlying neuronal population. This synchrony is co-ordinated by a balance between the activity of inhibitory and excitatory neurons and thus reflects phases of low versus high cortical excitability (Klimesch et al., 2007; Mathewson et al., 2011; Mazaheri and Jensen, 2010; Toscani et al., 2010). The consequence of these phasic cycles in inhibition/excitation is suppression/enhancement of interfering/relevant stimulus information (Busch et al., 2009; Ergenoglu et al., 2004; Hanslmayr et al., 2007; Linkenkaer-Hansen et al., 2004; Thut et al., 2006; Worden et al., 2000) and reduction/enhancement of PBR and NBR (Fig. 4). The phase of the alpha oscillation has also been shown to modulate the power of high frequency (>30 Hz) gamma activity (Osipova et al., 2008). Therefore a potential mechanism by which alpha indirectly modulates the PBR could be through the correlation between gamma activity and the BOLD signal which has been demonstrated invasively (Goense and Logothetis, 2008).

However, the neurophysiological origins of NBR remain incompletely understood (Goense et al., 2012), although both transcranial magnetic stimulation and neuroimaging studies have suggested that ipsilateral NBR reflects interhemispheric inhibition via reduction of excitatory input (Allison et al., 2000; Chen and Hallett, 1999; Kastrup et al., 2008; Klingner et al., 2011; Shmuel et al., 2002). The contribution of increased local inhibition to the local decrease in neuronal activity (Shmuel et al., 2006), as well as the frequency specificity of the decrease in neuronal activity potentially underlying the NBR, remain unknown.

An intrinsic, negative linear coupling between alpha-power and the BOLD signal during the resting-state has been widely demonstrated in visual cortex (de Munck et al., 2009; Goldman et al., 2002) and a positive alpha–BOLD coupling in the DMN has been recently reported (Mo et al., 2012). The reductions in neuronal activity (NBR) in auditory cortex that are observed during visual stimulation have been attributed to cross-modal inhibition (Kawashima et al., 1995; Laurienti et al., 2002; Mozolic et al., 2008). Long-range synchronisation of oscillatory rhythms between cortical regions has been shown to establish functional connectivity and facilitates the integration of information between cortical regions (Fries, 2005; Varela et al., 2001). Complementary to this, we have shown that the same regions of primary visual and primary auditory cortices where a significant interaction between alpha-power and the BOLD response to stimulation is observed, also display significant functional connectivity during the resting-state (Fig. 6), demonstrating a potential underlying functional substrate for the observed alpha–BOLD interaction. We hypothesize a functional relationship that links increases in alpha-power, inhibition and NBR amplitude where alpha-power acts as mediator for auditory inhibition, the strength of which is represented in part by NBR, as a mechanism to improve network processing and responses to the visual stimulation. We therefore observe that alpha-power indexes both short and long-range cortical excitability of visual and auditory cortex respectively.

Posterior alpha and rolandic mu power has been shown to reflect the excitability of visual and sensorimotor cortices respectively (Anderson and Ding, 2011; Neuper et al., 2006; Pineda, 2005; Reinacher et al., 2009; Romei et al., 2008; Steriade and Llinas, 1988; Worden et al., 2000; Zhang and Ding, 2010), but their link to the excitability of cortical networks beyond their sensory modality is little studied. An important topic for future research is to investigate how the functional interaction and collaboration between macroscale ICNs mediate brain function and behaviour. Auditory cortex is thought to possess its own bilateral ~10 Hz rhythm (Weisz et al., 2011) which would be expected to best index auditory excitability, though the convolutions of the cortical surface mean that this is poorly represented in scalp EEG. The presentation of a visual stimulus results in excitatory neuronal signalling propagating via the LGN to V1. During a state of enhanced alpha power this stimulation results in reduced visual positive BOLD and enhanced magnitude of auditory negative BOLD. Considering the functional and structural connectivity between visual and auditory cortices (Beer et al., 2011; Eckert et al., 2008; Falchier et al., 2002; Rockland and Ojima, 2003), we hypothesize that this increased alpha power and visual cortex excitability is associated with reduced excitatory input to auditory cortex (and auditory NBR) via cross-modal modulations of the intrinsic functional coupling between the cortices. Top–down modulation from frontal or parietal cortices

could also contribute to modulation of auditory cortex activity due to the increased attentional resources recruited by visual areas (Hopfinger et al., 2000).

Alpha and NBR relationships in the DMN

Pre-stimulus alpha-power also modulated NBR in midline DMN regions. The DMN is an anatomically organized mode of neuronal activity that is preferentially engaged during the resting-state (Buckner et al., 2008). The magnitude of DMN deactivation in response to stimulation has been shown to reflect the level of subject's task-engagement (McKiernan et al., 2006; Singh and Fawcett, 2008). Invasive electrophysiological recordings in humans demonstrate that DMN deactivation can be confidently interpreted as a decrease in local neuronal activity in response to stimulation (Miller et al., 2009). In the current study, increased pre-stimulus cortical excitability (lower alpha-power) is associated with a subsequently more engaging stimulus that evokes larger amplitude visual PBR, and results in a greater interruption of intrinsic processes and enhanced DMN deactivation, concurrent with increased inhibition of auditory cortex. Occipital alpha-power provides an index of subjects' alertness, arousal and cortical excitability that is indirectly related to the responsiveness of the DMN network to the visual stimulus. DMN fluctuations are posited to reflect either externally directed monitoring of the environment, or internally directed mentation (Buckner et al., 2008), both of which could be associated with fluctuations in subjects' susceptibility/responsiveness that would affect the saliency of an external stimulus. As such, the ongoing pattern of synchronisation/desynchronisation of alpha oscillations could in some circumstances be analogous to the fluctuations of activation/deactivation that are used to describe DMN function. In support of this hypothesis, a recent study (Mo et al., 2012) suggests that fluctuations in resting-state alpha power reflect the antagonistic relationship observed between the task-negative (DMN) and task-positive (fronto-parietal) networks with fMRI (Fox et al., 2005).

Conclusion

We used simultaneous EEG–fMRI to demonstrate a significant interaction between the amplitude of spontaneous alpha-power and the magnitude of both PBR and NBR to brief visual stimulation. We provide novel evidence that the spontaneous "baseline" of brain activity can substantially modulate the amplitude and shape of visual PBR and auditory and DMN NBR dependent upon stimulus properties. The modulated regions form a functionally connected network during the resting state. Our findings have important implications for measurements of brain activation using fMRI that are relative to a pre-stimulus baseline, particularly when interpreting how relative BOLD changes relate to the metabolic cost of switching between different states of brain activity.

Supplementary data to this article can be found online at http://dx.doi.org/10.1016/j.neuroimage.2013.02.070.

Acknowledgments

We thank the Engineering and Physical Science Research Council (EPSRC) for funding this research. APB: EP/F023057/1; SDM: EP/I022325/1.

Conflict of interest statement

The authors have no conflicts of interest.

References

Allison, J.D., Meador, K.J., Loring, D.W., Figueroa, R.E., Wright, J.C., 2000. Functional MRI cerebral activation and deactivation during finger movement. Neurology 54, 135–142.
Anderson, K.L., Ding, M., 2011. Attentional modulation of the somatosensory mu rhythm. Neuroscience 180, 165–180.
Arieli, A., Sterkin, A., Grinvald, A., Aertsen, A., 1996. Dynamics of ongoing activity: explanation of the large variability in evoked cortical responses. Science 273, 1868–1871.
Becker, R., Ritter, P., Villringer, A., 2008. Influence of ongoing alpha rhythm on the visual evoked potential. NeuroImage 39, 707–716.
Becker, R., Reinacher, M., Freyer, F., Villringer, A., Ritter, P., 2011. How ongoing neuronal oscillations account for evoked fMRI variability. J. Neurosci. 31, 11016–11027.
Beckmann, C.F., Smith, S.M., 2004. Probabilistic independent component analysis for functional magnetic resonance imaging. IEEE Trans. Med. Imaging 23, 137–152.
Beer, A.L., Plank, T., Greenlee, M.W., 2011. Diffusion tensor imaging shows white matter tracts between human auditory and visual cortex. Exp. Brain Res. 213, 299–308.
Berger, H., 1929. Uber das elektroenkephalogram des menschen. Arch. Psychiatr. Nevenkr. 87, 527–570.
Brookes, M.J., Gibson, A.M., Hall, S.D., Furlong, P.L., Barnes, G.R., Hillebrand, A., Singh, K.D., Holliday, I.E., Francis, S.T., Morris, P.G., 2005. GLM-beamformer method demonstrates stationary field, alpha ERD and gamma ERS co-localisation with fMRI BOLD response in visual cortex. NeuroImage 26, 302–308.
Buckner, R.L., Andrews-Hanna, J.R., Schacter, D.L., 2008. The brain's default network: anatomy, function, and relevance to disease. Ann. N. Y. Acad. Sci. 1124, 1–38.
Busch, N.A., Dubois, J., VanRullen, R., 2009. The phase of ongoing EEG oscillations predicts visual perception. J. Neurosci. 29, 7869–7876.
Chen, R., Hallett, M., 1999. The time course of changes in motor cortex excitability associated with voluntary movement. Can. J. Neurol. Sci. 26, 163–169.
De Luca, M., Beckmann, C.F., De Stefano, N., Matthews, P.M., Smith, S.M., 2006. fMRI resting state networks define distinct modes of long-distance interactions in the human brain. NeuroImage 29, 1359–1367.
de Munck, J.C., Gonçalves, S.I., Mammoliti, R., Heethaar, R.M., Lopes da Silva, F.H., 2009. Interactions between different EEG frequency bands and their effect on alpha–fMRI correlations. NeuroImage 47, 69–76.
Debener, S., Ullsperger, M., Siegel, M., Engel, A.K., 2006. Single-trial EEG–fMRI reveals the dynamics of cognitive function. Trends Cogn. Sci. 10, 558–563.
Eckert, M.A., Kamdar, N.V., Chang, C.E., Beckmann, C.F., Greicius, M.D., Menon, V., 2008. A cross-modal system linking primary auditory and visual cortices: evidence from intrinsic fMRI connectivity analysis. Hum. Brain Mapp. 29, 848–857.
Ergenoglu, T., Demiralp, T., Bayraktaroglu, Z., Ergen, M., Beydagi, H., Uresin, Y., 2004. Alpha rhythm of the EEG modulates visual detection performance in humans. Brain Res. Cogn. Brain Res. 20, 376–383.
Falchier, A., Clavagnier, S., Barone, P., Kennedy, H., 2002. Anatomical evidence of multimodal integration in primate striate cortex. J. Neurosci. 22, 5749–5759.
Ferbert, A., Priori, A., Rothwell, J.C., Day, B.L., Colebatch, J.G., Marsden, C.D., 1992. Interhemispheric inhibition of the human motor cortex. J. Physiol. 453, 525–546.
Fox, M.D., Snyder, A.Z., Vincent, J.L., Corbetta, M., Van Essen, D.C., Raichle, M.E., 2005. The human brain is intrinsically organized into dynamic, anticorrelated functional networks. Proc. Natl. Acad. Sci. U. S. A. 102, 9673–9678.
Fox, M.D., Snyder, A.Z., Vincent, J.L., Raichle, M.E., 2007. Intrinsic fluctuations within cortical systems account for intertrial variability in human behavior. Neuron 56, 171–184.
Foxe, J.J., Simpson, G.V., Ahlfors, S.P., 1998. Parieto-occipital approximately 10 Hz activity reflects anticipatory state of visual attention mechanisms. Neuroreport 9, 3929–3933.
Fries, P., 2005. A mechanism for cognitive dynamics: neuronal communication through neuronal coherence. Trends Cogn. Sci. 9, 474–480.
Friston, K.J., Buechel, C., Fink, G.R., Morris, J., Rolls, E., Dolan, R.J., 1997. Psychophysiological and modulatory interactions in neuroimaging. NeuroImage 6, 218–229.
Goense, J.B.M., Logothetis, N.K., 2008. Neurophysiology of the BOLD fMRI signal in awake monkeys. Curr. Biol. 18, 631–640.
Goense, J., Merkle, H., Logothetis, N.K., 2012. High-resolution fMRI reveals laminar differences in neurovascular coupling between positive and negative BOLD responses. Neuron 76, 629–639.
Goldman, R.I., Stern, J.M., Engel, J., Jerome, Cohen, M.S., 2002. Simultaneous EEG and fMRI of the alpha rhythm. Neuroreport 13, 2487–2492.
Hanslmayr, S., Aslan, A., Staudigl, T., Klimesch, W., Herrmann, C.S., Bauml, K.H., 2007. Prestimulus oscillations predict visual perception performance between and within subjects. NeuroImage 37, 1465–1473.
Hopfinger, J.B., Buonocore, M.H., Mangun, G.R., 2000. The neural mechanisms of top–down attentional control. Nat. Neurosci. 3, 284–291.
Hughes, S.W., Lorincz, M., Cope, D.W., Blethyn, K.L., Kekesi, K.A., Parri, H.R., Juhasz, G., Crunelli, V., 2004. Synchronized oscillations at alpha and theta frequencies in the lateral geniculate nucleus. Neuron 42, 253–268.
Hyvarinen, A., 1999. Fast and robust fixed-point algorithms for independent component analysis. IEEE Trans. Neural Netw. 10, 626–634.
Jenkinson, M., Smith, S., 2001. A global optimisation method for robust affine registration of brain images. Med. Image Anal. 5, 143–156.
Jenkinson, M., Bannister, P., Brady, M., Smith, S., 2002. Improved optimization for the robust and accurate linear registration and motion correction of brain images. NeuroImage 17, 825–841.
Jensen, O., Mazaheri, A., 2010. Shaping functional architecture by oscillatory alpha activity: gating by inhibition. Front. Hum. Neurosci. 4, 186.
Kastner, S., Schneider, K.A., Wunderlich, K., 2006. Beyond a relay nucleus: neuroimaging views on the human LGN. Prog. Brain Res. 155, 125–143.
Kastrup, A., Baudewig, J., Schnaudigel, S., Huonker, R., Becker, L., Sohns, J.M., Dechent, P., Klingner, C., Witte, O.W., 2008. Behavioral correlates of negative BOLD signal changes in the primary somatosensory cortex. NeuroImage 41, 1364–1371.
Kawashima, R., O'Sullivan, B.T., Roland, P.E., 1995. Positron-emission tomography studies of cross-modality inhibition in selective attentional tasks: closing the "mind's eye". Proc. Natl. Acad. Sci. U. S. A. 92, 5969–5972.

Klimesch, W., 1997. EEG-alpha rhythms and memory processes. Int. J. Psychophysiol. 26, 319–340.
Klimesch, W., Sauseng, P., Hanslmayr, S., 2007. EEG alpha oscillations: the inhibition-timing hypothesis. Brain Res. Rev. 53, 63–88.
Klingner, C.M., Hasler, C., Brodoehl, S., Witte, O.W., 2010. Dependence of the negative BOLD response on somatosensory stimulus intensity. NeuroImage 53, 189–195.
Klingner, C.M., Huonker, R., Flemming, S., Hasler, C., Brodoehl, S., Preul, C., Burmeister, H., Kastrup, A., Witte, O.W., 2011. Functional deactivations: multiple ipsilateral brain areas engaged in the processing of somatosensory information. Hum. Brain Mapp. 32, 127–140.
Laurienti, P.J., Burdette, J.H., Wallace, M.T., Yen, Y.F., Field, A.S., Stein, B.E., 2002. Deactivation of sensory-specific cortex by cross-modal stimuli. J. Cogn. Neurosci. 14, 420–429.
Linkenkaer-Hansen, K., Nikulin, V.V., Palva, S., Ilmoniemi, R.J., Palva, J.M., 2004. Prestimulus oscillations enhance psychophysical performance in humans. J. Neurosci. 24, 10186–10190.
Lorincz, M.L., Kekesi, K.A., Juhasz, G., Crunelli, V., Hughes, S.W., 2009. Temporal framing of thalamic relay-mode firing by phasic inhibition during the alpha rhythm. Neuron 63, 683–696.
Mathewson, K.E., Lleras, A., Beck, D.M., Fabiani, M., Ro, T., Gratton, G., 2011. Pulsed out of awareness: EEG alpha oscillations represent a pulsed-inhibition of ongoing cortical processing. Front. Psychol. 2.
Mayhew, S.D., Iannetti, G.D., Woolrich, M.W., Wise, R.G., 2006. Automated single-trial measurement of amplitude and latency of laser-evoked potentials (LEPs) using multiple linear regression. Clin. Neurophysiol. 117, 1331–1344.
Mazaheri, A., Jensen, O., 2010. Shaping functional architecture by oscillatory alpha activity: gating by inhibition. Front. Hum. Neurosci. 4, 186.
McKiernan, K.A., D'Angelo, B.R., Kaufman, J.N., Binder, J.R., 2006. Interrupting the "stream of consciousness": an fMRI investigation. NeuroImage 29, 1185–1191.
Miller, K.J., Weaver, K.E., Ojemann, J.G., 2009. Direct electrophysiological measurement of human default network areas. Proc. Natl. Acad. Sci. U. S. A. 106, 12174–12177.
Mo, J., Liu, Y., Huang, H., Ding, M., 2012. Coupling between visual alpha oscillations and default mode activity. NeuroImage 68C, 112–118.
Mozolic, J.L., Joyner, D., Hugenschmidt, C.E., Peiffer, A.M., Kraft, R.A., Maldjian, J.A., Laurienti, P.J., 2008. Cross-modal deactivations during modality-specific selective attention. BMC Neurol. 8, 35.
Mullinger, K.J., Bowtell, R., 2011. Combining EEG and FMRI. Meth. Mol. Biol. 711, 303–326.
Mullinger, K.J., Morgan, P.S., Bowtell, R.W., 2008. Improved artifact correction for combined electroencephalography/functional MRI by means of synchronization and use of vectorcardiogram recordings. J. Magn. Reson. Imaging 27, 607–616.
Neuper, C., Wörtz, M., Pfurtscheller, G., 2006. ERD/ERS patterns reflecting sensorimotor activation and deactivation. Prog. Brain Res. 159, 211–222.
Niazy, R.K., Beckmann, C.F., Iannetti, G.D., Brady, J.M., Smith, S.M., 2005. Removal of fMRI environment artifacts from EEG data using optimal basis sets. NeuroImage 28, 720–737.
Nierhaus, T., Schön, T., Becker, R., Ritter, P., Villringer, A., 2009. Background and evoked activity and their interaction in the human brain. Magn. Reson. Imaging 27, 1140–1150.
O'Connor, D.H., Fukui, M.M., Pinsk, M.A., Kastner, S., 2002. Attention modulates responses in the human lateral geniculate nucleus. Nat. Neurosci. 5, 1203–1209.
Oostenveld, R., Fries, P., Maris, E., Schoffelen, J.M., 2011. FieldTrip: open source software for advanced analysis of MEG, EEG, and invasive electrophysiological data. Comput. Intell. Neurosci. 2011, 156869.
O'Reilly, J.X., Woolrich, M.W., Behrens, T.E., Smith, S.M., Johansen-Berg, H., 2012. Tools of the trade: psychophysiological interactions and functional connectivity. Soc. Cogn. Affect. Neurosci. 7, 604–609.
Osipova, D., Hermes, D., Jensen, O., 2008. Gamma power is phase-locked to posterior alpha activity. PLoS One 3, e3990.
Ostwald, D., Porcaro, C., Bagshaw, A.P., 2010. An information theoretic approach to EEG–fMRI integration of visually evoked responses. NeuroImage 49, 498–516.
Ostwald, D., Porcaro, C., Bagshaw, A.P., 2011. Voxel-wise information theoretic EEG–fMRI feature integration. NeuroImage 55, 1270–1286.
Pineda, J.A., 2005. The functional significance of mu rhythms: translating "seeing" and "hearing" into "doing". Brain Res. Brain Res. Rev. 50, 57–68.
Porcaro, C., Ostwald, D., Bagshaw, A.P., 2010. Functional source separation improves the quality of single trial visual evoked potentials recorded during concurrent EEG–fMRI. NeuroImage 50, 112–123.
Raichle, M.E., MacLeod, A.M., Snyder, A.Z., Powers, W.J., Gusnard, D.A., Shulman, G.L., 2001. A default mode of brain function. Proc. Natl. Acad. Sci. U. S. A. 98, 676–682.
Reinacher, M., Becker, R., Villringer, A., Ritter, P., 2009. Oscillatory brain states interact with late cognitive components of the somatosensory evoked potential. J. Neurosci. Methods 183, 49–56.
Rockland, K.S., Ojima, H., 2003. Multisensory convergence in calcarine visual areas in macaque monkey. Int. J. Psychophysiol. 50, 19–26.
Romei, V., Brodbeck, V., Michel, C., Amedi, A., Pascual-Leone, A., Thut, G., 2008. Spontaneous fluctuations in posterior alpha-band EEG activity reflect variability in excitability of human visual areas. Cereb. Cortex 18, 2010–2018.
Scheeringa, R., Mazaheri, A., Bojak, I., Norris, D.G., Kleinschmidt, A., 2011. Modulation of visually evoked cortical fMRI responses by phase of ongoing occipital alpha oscillations. J. Neurosci. 31, 3813–3820.
Scheibe, C., Ullsperger, M., Sommer, W., Heekeren, H.R., 2010. Effects of parametrical and trial-to-trial variation in prior probability processing revealed by simultaneous electroencephalogram/functional magnetic resonance imaging. J. Neurosci. 30, 16709–16717.
Shmuel, A., Yacoub, E., Pfeuffer, J., Van de Moortele, P.F., Adriany, G., Hu, X., Ugurbil, K., 2002. Sustained negative BOLD, blood flow and oxygen consumption response and its coupling to the positive response in the human brain. Neuron 36, 1195–1210.
Shmuel, A., Augath, M., Oeltermann, A., Logothetis, N.K., 2006. Negative functional MRI response correlates with decreases in neuronal activity in monkey visual area V1. Nat. Neurosci. 9, 569–577.
Singh, K.D., Fawcett, I.P., 2008. Transient and linearly graded deactivation of the human default-mode network by a visual detection task. NeuroImage 41, 100–112.
Smith, S.M., 2002. Fast robust automated brain extraction. Hum. Brain Mapp. 17, 143–155.
Smith, S.M., Fox, P.T., Miller, K.L., Glahn, D.C., Fox, P.M., Mackay, C.E., Filippini, N., Watkins, K.E., Toro, R., Laird, A.R., Beckmann, C.F., 2009. Correspondence of the brain's functional architecture during activation and rest. Proc. Natl. Acad. Sci. U. S. A. 106, 13040–13045.
Steriade, M., Llinas, R.R., 1988. The functional states of the thalamus and the associated neuronal interplay. Physiol. Rev. 68, 649–742.
Thut, G., Nietzel, A., Brandt, S.A., Pascual-Leone, A., 2006. Alpha-band electroencephalographic activity over occipital cortex indexes visuospatial attention bias and predicts visual target detection. J. Neurosci. 26, 9494–9502.
Tootell, R.B., Hadjikhani, N., Hall, E.K., Marrett, S., Vanduffel, W., Vaughan, J.T., Dale, A.M., 1998. The retinotopy of visual spatial attention. Neuron 21, 1409–1422.
Toscani, M., Marzi, T., Righi, S., Viggiano, M.P., Baldassi, S., 2010. Alpha waves: a neural signature of visual suppression. Exp. Brain Res. 207, 213–219.
Varela, F., Lachaux, J.P., Rodriguez, E., Martinerie, J., 2001. The brainweb: phase synchronization and large-scale integration. Nat. Rev. Neurosci. 2, 229–239.
Weisz, N., Hartmann, T., Muller, N., Lorenz, I., Obleser, J., 2011. Alpha rhythms in audition: cognitive and clinical perspectives. Front. Psychol. 2, 73.
Woertz, M., Pfurtscheller, G., Klimesch, W., 2004. Alpha power dependent light stimulation: dynamics of event-related (de)synchronization in human electroencephalogram. Brain Res. Cogn. Brain Res. 20, 256–260.
Woolrich, M.W., Ripley, B.D., Brady, M., Smith, S.M., 2001. Temporal autocorrelation in univariate linear modeling of fMRI data. NeuroImage 14, 1370–1386.
Woolrich, M.W., Behrens, T.E., Beckmann, C.F., Jenkinson, M., Smith, S.M., 2004. Multilevel linear modelling for fMRI group analysis using Bayesian inference. NeuroImage 21, 1732–1747.
Worden, M.S., Foxe, J.J., Wang, N., Simpson, G.V., 2000. Anticipatory biasing of visuospatial attention indexed by retinotopically specific alpha-band electroencephalography increases over occipital cortex. J. Neurosci. 20, RC63.
Zhang, Y., Ding, M., 2010. Detection of a weak somatosensory stimulus: role of the prestimulus mu rhythm and its top–down modulation. J. Cogn. Neurosci. 22, 307–322.